BL College Journal
Full PDF
www.blcollege.edu.bd
ISSN 2664-228X (Print)
ISSN 2710-3684 (Online)
Volume -IV, Issue-I, July 2022
Pp. 140-155

Study of Nanocrystallization Kinetics in $Fe_{73.5}Cu_1Nb_3Si_{13.5}B_9$ Finemet Type Alloy by Differential Thermal Analysis and Using Different Models

Pritish Kumar Roy and Dr. Shibendra Shekher Sikder

Pritish Kumar Roy
Associate Professor
Department of Physics
Government Brajalal College
Khulna, Bangladesh
e-mail : pritish1974.phy@gmail.com

Dr. Shibendra Shekher Sikder
Professor, Department of Physics
Khulna University of
Engineering and Technology
(KUET), Bangladesh
e-mail : sssikder@phy.kuet.ac.bd

Abstract

The study of the crystallization processes in the FINEMET type nanocrystalline amorphous alloy is interesting not only from the fundamental aspect of establishing reaction mechanism of crystal nucleation and growth, but also from a technological point of view. The process and nature of crystallization phase constitution of nanocrystalline amorphous alloy of composition $Fe_{73.5}Cu_1Nb_3Si_{13.5}B_9$ prepared by rapid quenching method is investigated in the present study. The amorphous nature of the alloy has been verified by x-ray diffraction (XRD). The differential thermal analysis (DTA) experiments were performed at different continuous heating rates of 10, 20, 30, 40 and 50^0C/min. Two different crystalline phases are observed. The crystallization temperatures, the volume fraction of crystallizations and enthalpies of two different crystalline phases of the alloy have been determined from DTA traces. The dependence of on-set crystallization temperature (T_X) on the heating rate of different phases have been used for the determination of different crystallization parameters such as, the activation energy of crystallization, the order parameter or Avrami exponent (n). The results of crystallization were discussed on the basis of different models such as Kissinger's approach and modification for non-isothermal crystallization of Matusita in addition to Kolmogorov, Johnson, Mehl, Avrami and Ozawa.

Keywords

Amorphous, FINEMET, XRD, DTA, α-Fe(Si) phase, Fe_2B phase, Activation energy of crystallization, Avrami exponent.

1. Introduction

Traditionally, solid state physics has meant crystal physics. Solidity and crystallinity are considered as synonymous in text on condensed matter physics. Yet one of the most active fields of solid state research starts from the middle of the last century has been the study of solids that are not crystals, solids in which the arrangement of atoms lacks the slightest vestige of long range order. The advances that have been made in the physics and chemistry of these materials, which are known as amorphous solids or glasses, have been widely appreciated within research community.

Amorphous soft magnetic alloys are now well accepted and mature materials. At first the great interest in amorphous metals stems from the reports by Duwez et.al[1] on the preparation and properties of amorphous metallic alloys. Simpson and Brambley[2] appear to have been the first to point out that the amorphous alloys are expected to have no magnetocrystalline anisotropy and should have very low coercivity.

Nanocrystalline soft magnetic materials were first reported in 1988 by Yoshizawa, Oguma and Yamauchi[3]. Exploitation of this novel material in practical applications started shortly after the discovery and manufactured by Hitachi Co. Ltd. under the trade name FINEMET[4]. FINEMET is the first nanocrystalline soft magnetic material in the world developed by Hitachi Metals, Ltd. The precursor material of FINEMET is amorphous metal obtained by rapid quenching the molten metal, consisting of Fe, Si, B and small amounts of Cu and Nb. The originally proposed composition of the alloy was $Fe_{73.5}Cu_1Nb_3Si_{13.5}B_9$. By applying proper heat treatment to the alloy at higher temperature (around 555^0C) than its crystallization temperature of the amorphous state, this alloy produces homogeneous, ultrafine nanocrystalline grain structure of α-Fe(Si) with bcc structure having grain diameter approximately 10 nanometer and gain unique soft magnetic properties[5]. Usually on crystallization of amorphous alloys much larger grains with diameter 0.1-1μm is obtained. The formation of this nanocrystalline structure is ascribed to the combined condition of Cu and Nb, which both are not soluble in α-Fe. Hereby Cu is thought to increase the nucleation of α-Fe grains, whereas Nb lowers its growth rate[6]. FINEMET has high saturation magnetic flux density (more than 1T) comparable to Fe-based metal and high permeability (10000 at 100kHz) comparable to Co-based amorphous metal. It has the advantages of both Fe-based and Co-based amorphous metals. Researchers are working on nanocrystalline soft magnetic

alloys since last around five decades. The interest has been growing day by day in the synthesis and characterization of FINEMET type nanocrystalline amorphous alloys due to their excellent performance in electromagnetic noise suppression and contribution to energy saving. It allows reduction in size and weight of electric and electronic devices. Magnetically soft materials are needed for the applications of magnetic devices such as transformer, inductive devices, biomedical applications, space applications and many more other applications. Nowadays, researchers are thinking that by using the nanoscience and technology, it is possible to solve many unsolved real life problems such as the fatal diseases like cancer.

FINEMET is obtained by the proper heat treatment to the amorphous state of the nanocrystalline alloy. So, study of crystallization kinetics and behavior of this type of fine metal (FINEMET) is fundamentally important. Differential thermal analysis (DTA) is a direct and effective technique for analyzing the crystallization kinetics and stability of the crystalline phase with respect to the crystallization process. In this technique structural change occurs in the material under heat treatment. These changes may be due to melting, solidification, dehydration, phase transition from glass to solid, transition from one crystalline variety to another, destruction of crystalline lattice, oxidation, decomposition etc. Differential thermal analysis (DTA) has been widely used in scientific and engineering fields to study clays, soaps, polymers and various other organic and inorganic materials those, may be solid or liquid. The DTA technique was first suggested by H. Le Chatelier[7] in 1887 and was applied to the study of clays and ceramics. The objectives of these DTA studies, generally speaking, included two aspects: identifying the characteristic temperature and nature of phase transformations of the alloy studied, and determining the effect of chemical composition and processing on phase transformation behavior in the alloy.

2. Experimental

Glassy alloy $Fe_{71.5}Cr_2Cu_1Nb_3Si_{13.5}B_9$ is prepared by melt spinning technique. The melt spinning facilities were used at the Centre for Materials Science, National University of Hanoi, Vietnam. Melt spinning is a widely used production method for rapidly solidifying materials as well as preparing amorphous metallic ribbons. Amorphous ribbons with the composition $Fe_{71.5}Cr_2Cu_1Nb_3Si_{13.5}B_9$ were prepared in an arc furnace on a water-cooled copper hearth under an atmosphere of pure Argon (Ar). High purity

(99.9%) source materials were obtained from Johnson Matthey (Alfa Aesar Inc.).

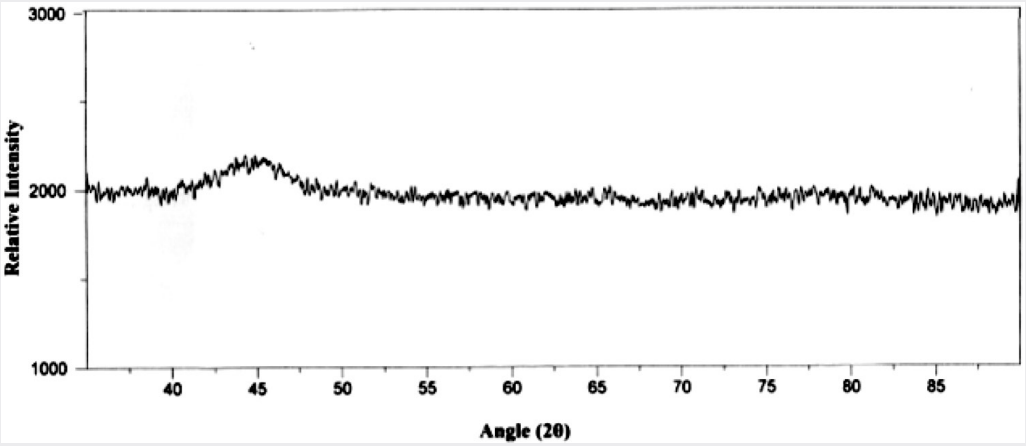

Fig. 1 XRD pattern of nanocrystalline amorphous $Fe_{71.5}Cr_2Cu_1Nb_3Si_{13.5}B_9$ alloy at room temperature.

A Philips Model PW 3040 X' Pert PRO XRD system was employed for studying the structure of the material. The copper target was used as a source of X-rays with λ = 1.5406 Å (Cu-K_α). The scanning angle was in the range of 30^0- 90^0. Fig. 1 shows the X-ray diffraction pattern of $Fe_{71.5}Cr_2Cu_1Nb_3Si_{13.5}B_9$ nanocrystalline amorphous ribbon at room temperature. The absence of any sharp structural peak confirms the amorphous nature of the sample.

Differential Thermal Analyzer (DTA) Shimadzu model TG/TDTA 6300 was used to measure the thermal manifestation of the phase transformation and to study the crystallization kinetics under non-isothermal condition. The DTA runs have been taken at five different heating rates i.e. 10, 20, 30, 40 and 50^0C/min on accurately weighed samples taken in aluminum pan. The temperature range covered in DTA was from room temperature to 800^0C.

3. Results and Discussion

In Fig. 2 DTA trace of as-cast nanocrystalline amorphous $Fe_{71.5}Cr_2Cu_1Nb_3Si_{13.5}B_9$ ribbon sample recorded in a nitrogen atmosphere with a heating rate of 10^0C/min has been presented.

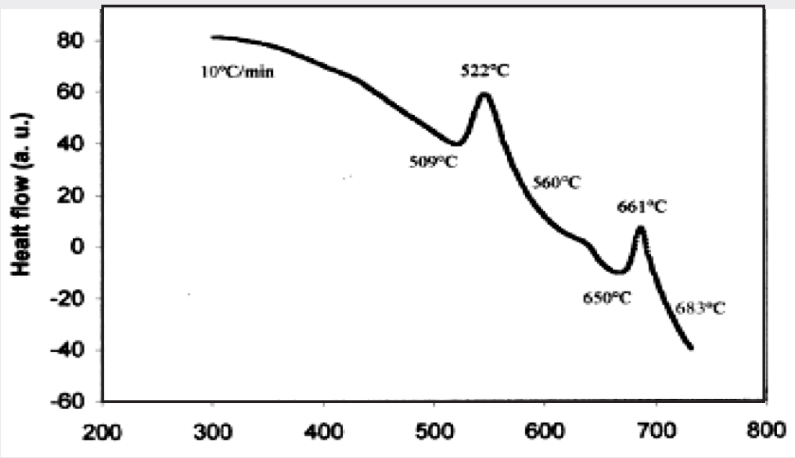

Fig. 2 DTA trace of as-cast nanocrystalline amorphous $Fe_{71.5}Cr_2Cu_1Nb_3Si_{13.5}B_9$ alloy.

There are clearly two separated exothermal peaks at T_{p1}=522^{0}C and T_{p2}=661^{0}C on DTA curve, ascribed to the precipitation of bcc-Fe(Si) and boride (FeB/Fe_2B) phase, respectively. Fig. 3 represents the DTA traces of as-cast nanocrystalline amorphous $Fe_{71.5}Cr_2Cu_1Nb_3Si_{13.5}B_9$ alloy from room temperature to 800^{o}C with heating rates of 10-50^{o}C/min at the step of 10^{o}C. In each DTA curve, two exothermic peaks are distinctly observed; corresponding to two different crystallization events initiated at temperature T_{x1} and T_{x2} respectively.

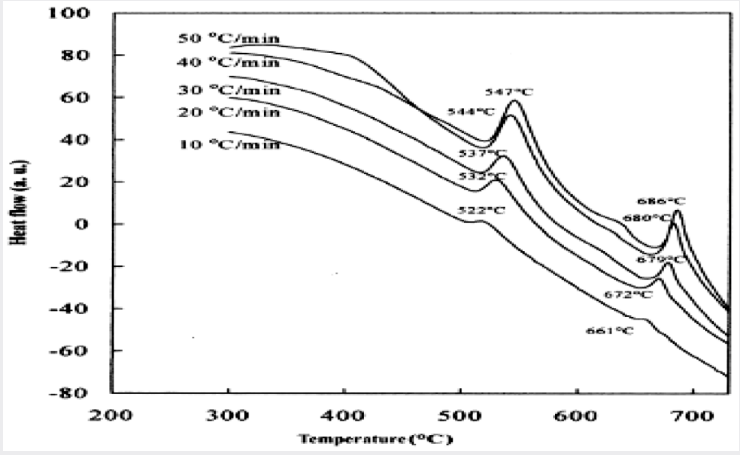

Fig. 3 Effects of heating rate on DTA trace of as-cast nanocrystalline amorphous $Fe_{71.5}Cr_2Cu_1Nb_3Si_{13.5}B_9$ alloy.

The on-set crystallization temperature T_x has been defined as temperature corresponding to the intersection of two linear portion adjoining the transition elbow of the DTA trace in the exothermic direction. The value of on-set crystallization temperatures (T_{x1} and T_{x2}), crystallization peak temperatures (T_{p1} and T_{p2}) and crystallization ending or completion temperatures (T_{e1} and T_{e2}) at different heating rates for the alloy is given in Table-1.

Table-1 Effects of heating rate on 1st and 2nd crystallization states of the nanocrystalline $Fe_{71.5}Cr_2Cu_1Nb_3Si_{13.5}B_9$ amorphous alloy.

Heating rate (β) in °C/min	1st crystallization state				2nd crystallization state				$(T_{p2}-T_{p1})$ in °C
	Onset temp. (T_{x1}) in °C	Peak temp. (T_{p1}) in °C	Ending temp. (T_{e1}) in °C	Temp. range ($T_{e1}-T_{x1}$) in °C	Onset temp. (T_{x2}) in °C	Peak temp (T_{p2}) in °C	Ending temp. (T_{e2}) in °C	Temp. range ($T_{e2}-T_{x2}$) in °C	
10	509	522	560	51	650	661	683	33	139
20	516	532	574	58	657	672	696	39	140
30	518	537	578	60	661	679	707	46	142
40	520	544	587	67	665	680	709	44	136
50	522	547	600	78	668	686	713	45	139

Fig. 3 reveals that the crystallization of each phase occurs over a wide range of temperatures and this temperature range increases with the increase of heating rate for the1st crystallization state, but a little anomaly is seen in the 2nd crystallization state. From Table-1 the crystallization temperature range for the 1st crystallization state is 51 to 78°C and for the 2nd crystallization state is 33 to 46°C. Crystallization temperature range for the 1st crystallization state is always greater than the 2nd crystallization state. The DTA curves in Fig. 3 show sharp peaks at 522-547°C for the 1st crystallization state depending on the heating rate from 10°C/min to 50°C/min, which is lower than that for original FINEMET 540-572°C respectively[8] and the replacement of 1% Fe by Cr of the original FINEMET 542-569°C respectively[9]. Fig. 3 also reveals that the peak temperature shifts to higher values with the increase of heating rate. In other word, more heat energy is required for the formation of crystalline phases with increasing heating rates. Table-1 also shows that the two crystallization events are separated by a large temperature gap of ~140°C. For FINEMET without Cr i.e. for pure FINEMET the temperature difference between two events was found ~150°C[10]. The large separation between two crystallization events is one of the characteristic features of the FINEMET type alloys, which exhibit easy nanocrystallization[11]. From Fig. 3 we can also see that

the peaks of 2nd crystallization state exhibited with high sharpness than the peaks of 1st crystallization state relating to strong crystallization of boride phase. These results are fully agreed with those reported in the work of C. Gomez-Polo et.al [12].

The crystallization volume fraction (α) at any temperature T is given as $\alpha = A_T/A$, where, A is the total area of exothermic peak between the on-set crystallization temperature T_x, where crystallization just begins and the temperature T_e where the crystallization peaks end i.e. crystallization is completed. A_T is the partial area of exothermic peak between the temperature T_x and T_e. The temperature T is selected between T_x and T_e.

The calculated values of volume fraction of crystallization at different heating rates for the alloy under study are listed in the Table-2.

Table -2 Effects of heating rate on crystallization volume fraction of 1st and 2nd crystallization states of the nanocrystalline $Fe_{71.5}Cr_2Cu_1Nb_3Si_{13.5}B_9$ amorphous alloy.

Heating rate (β) in ^{0}C/min	1st crystallization state			2nd crystallization state		
	Total peak area(A) in mm^2	Partial peak area(A_T) in mm^2	Crystallization volume fraction(α)	Total peak area(A) in mm^2	Partial peak area(A_T) in mm^2	Crystallization volume fraction(α)
10	9.53	2.55	0.27	5.66	1.26	0.22
20	16.98	5.48	0.32	8.90	3.12	0.35
30	15.92	6.01	0.34	13.80	5.19	0.38
40	23.86	10.62	0.45	18.05	8.79	0.49
50	41.38	20.55	0.50	21.98	11.8	0.54

Table-2 along with the Fig. 3 shows that the total peak area increases with the increase of heating rate for both the crystallization states and for each of the DTA trace, the area under the first crystallization peak is larger than the area covered by the second crystallization peak. Table-2 also shows that, the crystallization volume fraction (α) increases with the increase of heating rate for both the crystallization states. The dependence of on-set crystallization temperature (T_x) on the heating rate (β) is given by the empirical relation that has been suggested by Lasocka[13] and has the form:

$$T_x = B_x \ln \beta + A_x \quad (1)$$

Where, A_x and B_x are constants. The plots of ln(β) vs T_x for the 1st and 2nd crystallization states of the alloy is shown in Fig. 4(a) and Fig. 4(b).

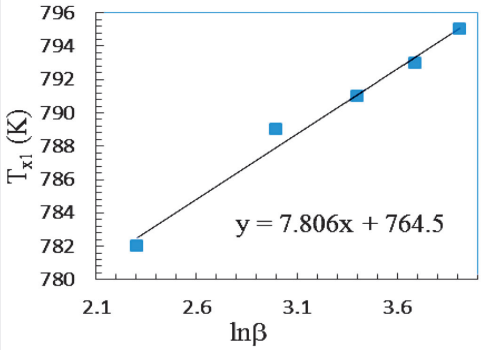

Fig. 4(a) Plot of T_{x1} [K] as a function of lnβ for α-Fe(Si) phase of $Fe_{71.5}Cr_2Nb_3Cu_1Si_{13.5}B_9$ alloy.

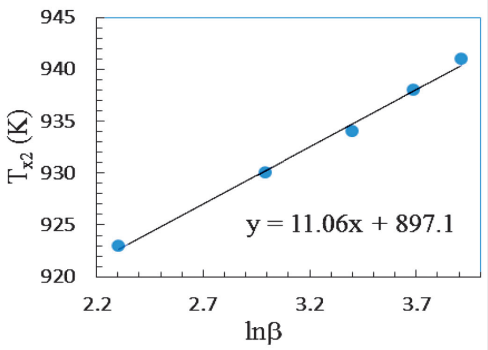

Fig. 4(b) Plot of T_{x2} [K] as a function of lnβ for Fe_2B phase of $Fe_{71.5}Cr_2Nb_3Cu_1Si_{13.5}B_9$ alloy.

The straight lines show the good validity of this relationship for the alloy. The calculated values of A_x =764.5K=491.5°C, B_x=7.81min for the 1st crystallization state and A_x =897.1K=624.1°C, B_x=11.06 min for the 2nd crystallization state. A_x values depict the crystallization temperature at a heating rate of 1^0C/min while B_x values are proportional to the time taken by the system to reduce its crystallization temperature when its heating rate is lowered from 10^0C/min to 1^0C/min.

The kinetics of isothermal crystallization involving nucleation and growth is usually analyzed using the Kolmogorov-Johnson-Mehl-Avrami (KJMA) model[14, 15]. According to this model, the volume fraction of crystallites ((0<α<1)) is given by[16-18]:

$$\alpha(t) = 1 - \exp\{-(kt)^n\} \quad (2)$$

where, α(t) is the volume fraction crystallized after time t, n is the Avrami exponent that is associated with the nucleation and growth mechanisms and k is the effective overall reaction rate, which actually reflects the rate of crystallization in thermally activated process and usually assigned Arrhenian temperature dependence,

$$k = k_0 \exp(-E_c/RT) \quad (3)$$

Where, E_c is the activation energy of crystallization, k_0 is the pre-exponential factor or frequency factor, which indicates the number attempts made by nuclei to overcome the energy barrier during crystallization and R is the gas constant. In the framework of KJMA model, the kinetic parameters n, k_0 and E_c are assumed to be constant during the crystallization process.

In non-isothermal crystallization, the existence of a constant heating rate condition is assumed. The relation between the sample temperature and the heating rate can be written as

$$T = T_0 + \beta t \tag{4}$$

Where, T_0 is the initial temperature and β is the heating rate. As the temperature constantly changes with time, k is no longer a constant but varies with time in a more complicated form and Eq. (2) becomes

$$\alpha\,(t) = 1 - \exp\,[-\{k\,(T-T_0)/\beta\}^n] \tag{5}$$

After rearranging and taking logarithms of Eq. (5), Ozawa[19, 20] obtained

$$\ln\,\{-\ln\,(1-\alpha)\} = n\ln k\,(T-T_0) - n\ln\beta \tag{6}$$

According to Eq. (6), a plot of $\ln\{-\ln(1-\alpha)\}$ versus $\ln\beta$ yield a straight line with slope equal to n.

Fig. 5(a) and Fig. 5(b) show the variation of $\ln\{-\ln(1-\alpha)\}$ against $\ln\beta$ for the nanocrystalline $Fe_{71.5}Cr_2Cu_1Nb_3Si_{13.5}B_9$ amorphous alloy. The value of n for the α-Fe(Si) crystalline phase is 0.60~1 and for the Fe_2B crystalline phase is 0.69~1.

It is well known that crystallization of nanocrystalline amorphous alloy is associated with nucleation and growth processes and the extent of crystallization increases with an increase in temperature. Due to these order parameter (n) changes. Since for the sample prepared by melt quenching technique, the value of n may be 4, 3, 2 or 1, which can be

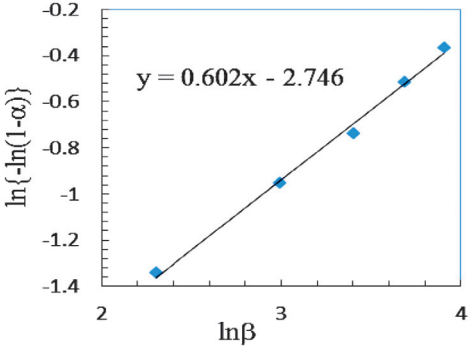

Fig. 5(a) Plot of $\ln\{-\ln(1-\alpha)\}$ as a function of $\ln\beta$ for the α-Fe(Si) phase of the $Fe_{71.5}Cr_2Nb_3Cu_1Si_{13.5}B_9$ alloy.

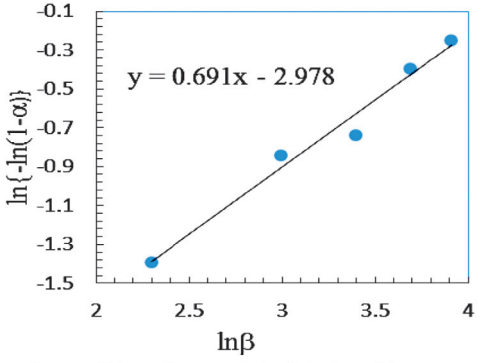

Fig. 5(b) Plot of $\ln\{-\ln(1-\alpha)\}$ as a function of $\ln\beta$ for the Fe_2B phase of the $Fe_{71.5}Cr_2Nb_3Cu_1Si_{13.5}B_9$ alloy.

related to different crystallization mechanism; n=4 represents volume nucleation, three dimensional growth; n=3 represents volume nucleation, two dimensional growth; n=2 represents volume nucleation, one dimensional growth; n=1 represents surface, one dimensional growth from surface to inside[21]. In our present system of nanocrystalline $Fe_{71.5}Cr_2Cu_1Nb_3Si_{13.5}B_9$ amorphous alloy, the value of n is equal to 1 for both the crystalline phase, which represents surface, one dimensional growth from surface to inside.

The interpretation of the experimental crystallization data is given on the basis of Kissinger's, modified Ozawa's and Matusita's equations for non-isothermal crystallization. The activation energy (E_c) for crystallization can therefore be calculated by using Kissinger's equation[22],

$$\ln (\beta/T_p^2) = - E_c / RT_p + C \qquad (7)$$

Where, C is a constant.

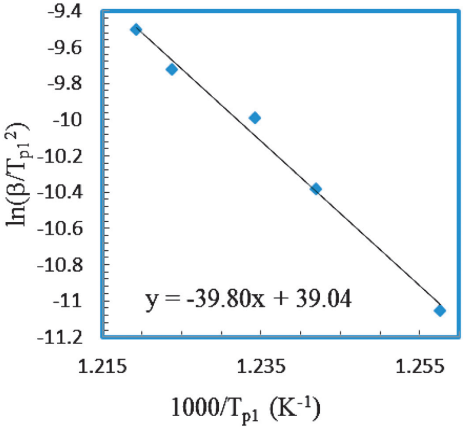

Fig. 6(a) Plot of $\ln(\beta/T_{p1}^2)$ as a function of $1000/T_{p1}$ $[K^{-1}]$ for the α-Fe(Si) phase of the $Fe_{71.5}Cr_2Nb_3Cu_1Si_{13.5}B_9$ alloy.

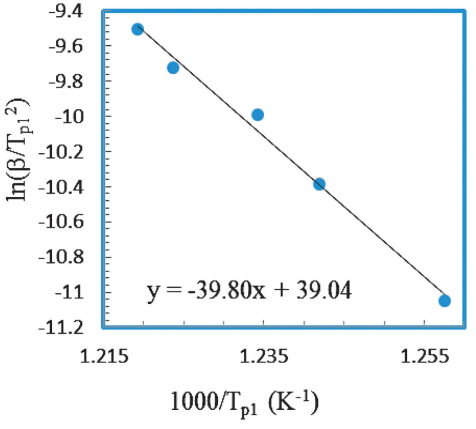

Fig. 6(b) Plot of $\ln(\beta/T_{p2}^2)$ as a function of $1000/T_{p2}$ $[K^{-1}]$ for the Fe_2B phase of the $Fe_{71.5}Cr_2Nb_3Cu_1Si_{13.5}B_9$ alloy.

The plots of $\ln(\beta/T_p^2)$ versus $1000/T_p$ for nanocrystalline $Fe_{71.5}Cr_2Cu_1Nb_3Si_{13.5}B_9$ amorphous alloy are shown in Fig. 6(a) and Fig. 6(b), which come to be straight lines. The value of E_c may be calculated from the slope of each line and it is found for the α-Fe(Si) crystalline phase is 3.43eV and for the Fe_2B crystalline phase is 4.92eV.

The activation energy of crystallization can be obtained from the variation of the crystallization peak temperature with heating rate by using Ozawa's[20] relation as :

$$\ln \beta = E_c / RT_p + D \qquad (8)$$

Where, D is a constant.

Fig. 7(a) and Fig. 7(b) show lnβ versus $1000/T_p$ dependences for the alloy under study, which come to be linear. The value of E_c is calculated from the slope of each line and it is found for the α-Fe(Si) crystalline phase is 3.57eV and for the Fe_2B crystalline phase is 5.08eV.

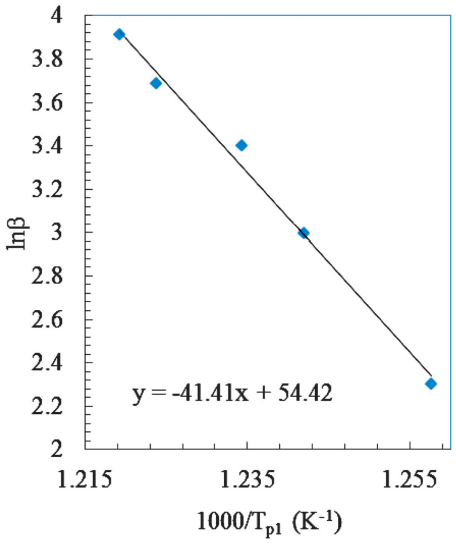

Fig. 7(a) Plot of lnβ as a function of $1000/T_{p1}$ $[K^{-1}]$ for the α-Fe(Si) phase of the $Fe_{71.5}Cr_2Nb_3Cu_1Si_{13.5}B_9$ alloy.

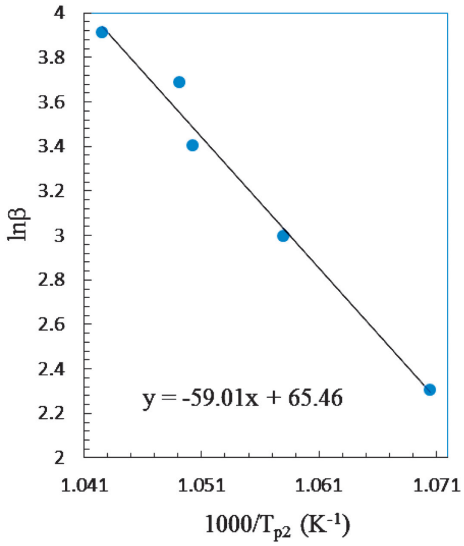

Fig. 7(b) Plot of lnβ as a function of $1000/T_{p2}$ $[K^{-1}]$ for the Fe_2B phase of the $Fe_{71.5}Cr_2Nb_3Cu_1Si_{13.5}B_9$ alloy.

The activation energy of crystallization can also be obtained from the variation of crystallization volume fraction (α) and the crystallization peak temperature with constant heating rates by using Matusita's[23] relation as:

$$\ln \{-\ln(1-\alpha)\} = -n \ln\beta - 1.052mEc / RT_p + \text{constant}$$

$$-[\ln \{-\ln(1-\alpha)\} + n \ln\beta] = 1.052mEc / RT_p - \text{constant} \qquad (9)$$

Where, m and n are integer or half integer numbers that depend on the growth mechanism and the dimensionality of the crystal. Usually it is considered m=1, 2 or 3 for one, two, or three dimensional growth of the crystal[24].

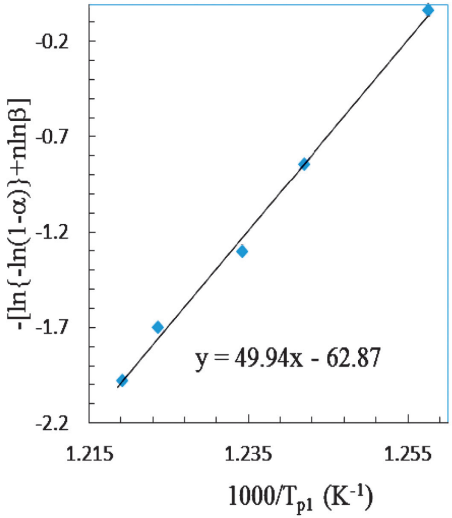

Fig. 8(a) Plot of -[ln-{ln(1-α)}+lnβ] as a function of $1000/T_{p1}$ [K^{-1}] for the α-Fe(Si) phase of the $Fe_{71.5}Cr_2Nb_3Cu_1Si_{13.5}B_9$ alloy.

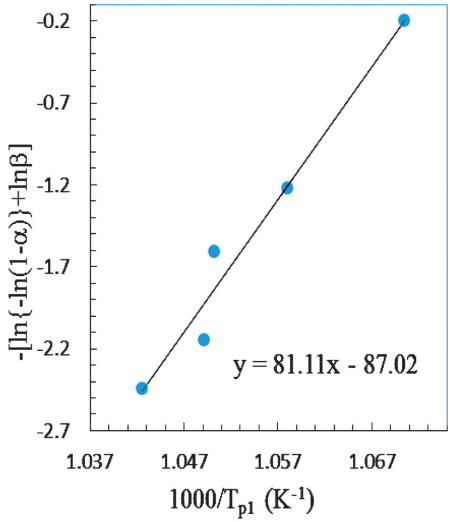

Fig. 8(b) Plot of -[ln-{ln(1-α)}+lnβ] as a function of $1000/T_{p2}$ [K^{-1}] for the Fe_2B phase of the $Fe_{71.5}Cr_2Nb_3Cu_1Si_{13.5}B_9$ alloy.

Fig. 8(a) and Fig. 8(b) show -[ln{-ln(1-α)}+ n lnβ] versus $1000/T_p$ dependences for the alloy under study, which come to be linear. The value of E_c is calculated from the slope of each line and it is found for the α-Fe(Si) crystalline phase is 4.09eV and for the Fe_2B crystalline phase is 6.65eV.

The values of the activation energy calculated from Eq. (8)[20] are slightly higher than the values of activation energy calculated from Eq. (7)[22]. So it can be considered Eq. (7) and Eq. (8) are in good agreement with each other. But, the value of the activation energy calculated from Eq. (9)[23] is a little bit higher.

The activation energy of the original FINEMET, the replacement of 1% Fe by Cr of the original FINEMET and the replacement of 2% Fe by Cr of the original FINEMET is listed in Table-3

Table-3 Activation energies of original FINEMET and modified FINEMET alloys.

FINEMET and modified FINEMET type alloys	Activation energy of 1st crystallization phase in eV	Activation energy of 2nd crystallization phase in eV	Model used for calculating activation energy of crystallization phases
$Fe_{73.5}Cu_1Nb_3Si_{13.5}B_9$	3.25[8]	-----	Kissinger's model
$Fe_{72.5}Cr_1Cu_1Nb_3Si_{13.5}B_9$	3.26[9]	4.87[9]	Kissinger's model
$Fe_{71.5}Cr_2Cu_1Nb_3Si_{13.5}B_9$	3.43 (present work)	4.92 (present work)	Kissinger's model
$Fe_{71.5}Cr_2Cu_1Nb_3Si_{13.5}B_9$	3.57 (present work)	5.08 (present work)	Ozawa's model
$Fe_{71.5}Cr_2Cu_1Nb_3Si_{13.5}B_9$	4.09 (present work)	6.65 (present work)	Matusita's model

The activation energy for formation of 1st crystallization α-Fe(Si) phase of the original FINEMET is 3.25eV[8, 22]. The activation energy of 1st crystallization phase of modified FINEMET type alloy $Fe_{72.5}Cr_1Cu_1Nb_3Si_{13.5}B_9$ (replacement of 1% Fe by Cr of the original FINEMET) is 3.26eV[9, 22], which is approximately similar to that of original FINEMET. But the activation energy of crystallization phases of modified FINEMET type alloy $Fe_{71.5}Cr_2Cu_1Nb_3Si_{13.5}B_9$ (replacement of 2% Fe by Cr of the original FINEMET) is 3.43eV[22], which is slightly higher than the previously observed tendency. It is also noticed that the activation energy for first crystallization phase is lower than the second crystallization phase. This is because, at the early stage of crystallization, a formation of Cu clusters leads to low activation energy for preferential nucleation however, with the increase of crystallized volume fraction, the Cu-rich regions gradually run out[25].

Measuring the total area under the exothermic peak, the experimental determination of crystallization enthalpy released ΔH_c during crystallization process is evaluated by using the formula:

$$\Delta H_c = KA / M \qquad (10)$$

Where, K is the constant of the instrument used, M is the mass of the sample and A is the area under the crystallization peak. Mass of the sample M was taken constant trough out the DTA experiment. So, from Eq. (10) it shows that, crystallization enthalpy released ΔH_c is directly proportional to the area under the crystallization peak. The value of ΔH_c i.e. the area under the crystallization peak for nanocrystalline $Fe_{71.5}Cr_2Cu_1Nb_3Si_{13.5}B_9$ amorphous alloy at different heating rates are shown in Table-2. From Table-2 it is seen that, enthalpy released for both the crystalline states increases with the increase of heating rate and the enthalpy released in 1st crystallization phase is higher than the

enthalpy released for 2nd crystallization phase. The release of enthalpy is related to the metastability of the crystalline phases and the least stable crystalline states are supposed to have maximum ΔH_c [21]. From the enthalpy consideration the 1st crystallization phase is less stable than the 2nd crystallization phase and both the phases have higher stability at the lower heating rate of the alloy under study.

4. Conclusions

Non-isothermal DTA measurements have been performed from room temperature to 800^0C at several heating rates in order to study the kinetics of the nanocrystallization process of the $Fe_{71.5}Cr_2Cu_1Nb_3Si_{13.5}B_9$ amorphous alloy. Replacement of 2% Fe by Cr of the original FINEMET was observed to decrease heating rate dependence crystallization (on-set or peak) temperature with respect to the original FINEMET and the FINEMET with the replacement of 1% Fe by Cr. Cr additions also narrowing the interval between crystallization (on-set or peak) temperatures of the observed crystallization states. A temperature interval of ~140°C between the two crystallization events is measured. This temperature gap is an indication of the enhancement of stability of α-Fe(Si) phase against detrimental Fe_2B phase due to a slight substitution of Cr in place of Fe. The nanocrystallization kinetics is described using the Kolmogorov-Johnson-Mehl-Avrami (KJMA) approach and values close to 1 were found for the Avrami exponent (n) for both the crystallization states of the alloy. The n values close to 1 are related to an increase of a diffusion barrier, suggesting a controlled diffusion process with a nucleation rate close to zero. The interpretation of the experimental crystallization data is given on the basis of M. Lasocka's, Kissinger's, modified Ozawa's and Matusita's equations. By employing Kissinger's, Ozawa's and Matusita's methods, the activation energy of crystallization (E_c) determined from the heating rate dependence of crystallization temperature. The activation energy of the primary crystallization of α-Fe(Si) phase is found to be 3.43eV(Kissinger), 3.57eV(Ozawa) and 4.09eV(Matusita). The results obtained from Kissinger's and Ozawa's models are very close to each other and compatible with the previous works which indicates that these two models are in good agreement with each other. The result obtained from Matusita's equation is a little bit higher. The activation energy is found to be increased with the increase of replacement amount of Fe by Cr. The results of crystallization kinetics indicate that the degree of crystallization fits well with the theory of Kolmogorov-Johnson-Mehl-Avrami (KJMA), Kissinger and Ozawa.

Acknowledgements

The authors are indebted to Centre for Materials Science, National University of Hanoi, Vietnam for sample supplies. The authors are also highly grateful to Bangladesh Council of Scientific and Industrial Research (BCSIR) and Atomic Energy Centre, Dhaka (AECD) for giving their experimental facilities. The first author specially grateful to all the teachers, colleagues and staffs of Department of Physics, Khulna University of Engineering and Technology (KUET) and Department of Physics, Government Brajalal College, Khulna for their vital support and inspiration.

References

[1] Pol Duwez, R. H. Willens and W. Klement jr, Continuous Series of Metastable Solid Solutions in Silver-Copper Alloys, *Journal of Applied Physics, 31*, 1960, p. 1136.

[2] A. W. Simpson and D. R. Brambley, The Magnetic and Structural Properties of Bulk Amorphous and Crystalline Co-P Alloys, *Physica Status Solidi (b) Vol. 43*, *Issue 1*, 1971, p. 291-300.

[3] Y. Yoshizawa, S. Oguma and K. Yamauchi, New Fe-based soft magnetic alloys composed of ultra-fine grain structure, *J. Appl. Phys. 64*, 1988, p. 6044-6046.

[4] Y. Yoshizawa & K. Yamauchi, Effects of Magnetic Field Annealing on Magnetic Properties in Ultrafine Crystalline Fe-Cu-Nb-Si-B Alloys, *IEEE Trans. Magnetics. 25*, 1989, p. 3324.

[5] Hitachi Metals, Ltd., http://www. Hitachi-metals.co.jp

[6] G. Herzer, Grain Structure and Magnetism of Nanocrystalline Ferromagnets, *IEEE Trans. Magnetics, MAG- 25*, 1989, p. 3327- 3328.

[7] H. Le Chatelier, The Constitution of Clay, *Z. Physik. Chem. I*, 1887, p. 396.

[8] Chau N, Hoa NQ, Luong NH., The crystallization in Finemet with Cu substituted by Ag, *Journal of Magnetism and Magnetic Materials, 290–291*, 2005, p. 1547–1550.

[9] Shihab MT, Reza MA, Shil SK, Tawhid MM, Sikder SS and Gafur MA, Study of crystallization phases and magnetic properties of nanocrystalline $Fe_{73.5}Cu_1Nb_3Si_{13.5}B_9$ alloy prepared by rapid quenching method, *Material Science & Engineering International Journal, Vol. 4, Issue 2*, 2020, p. 37- 43.

[10] Leu MS, Chin TS. Crystallization behavior and temperature dependence of the initial permeability of FeCuNbSiB alloy, *J Appl. Phys. 81*, 1997, p. 4051- 4053.

[11] G. Pozo López, L. M. Fabietti, A. M. Condó and S. E. Urreta, Microstructure and soft magnetic properties of Finemet-type ribbons obtained by twin-roller melt-spinning.

Journal of Magnetism and Magnetic Materials, Vol. 322, *Issue 20*, 2010, p. 3088-3093.

[12] C. Gomez-Polo, J.I. Perez-Landazabal, V. Recarte, *IEEE Transactions of Magnetics, Vol. 39*, *issue: 5*, 2003, p. 3019-3024.

[13] Maria Lasocka, The effect of scanning rate on glass transition temperature of splat-cooled $Te_{85}Ge_{15}$, *Materials Science and Engineering, Vol. 23*, *Issues: 2-3*, 1976, p. 173-177.

[14] A.N. Kolmogorov, Statistical theory of Nucleation processes, *Bull. Acad. Sci. U.S.S.R., Phys. Ser. 3*, 1937, p. 555.

[15] W. A. Johnson, R. F. Mehl, Reaction kinetics in processes of nucleation and growth, *Trans. Am. Inst. Min. Metall. Eng. 135,* 1939, p. 416-443.

[16] M. Avrami, Kinetics of phase change. I General theory, *Journal of Chemical Physics, Vol. 7*, *No. 12*, 1939, p. 1103-1113.

[17] M. Avrami, Kinetics of phase change II Transformation –time relations for random distribution of nuclei, *Journal of Chemical Physics, Vol. 8*, 1940, p. 212-224.

[18] M. Avrami, Kinetics of phase change III Granulation, phase change and microstructure, *Journal of Chemical Physics, Vol. 9*, 1941, p. 177-184.

[19] T. Ozawa, Kinetics of non-isothermal crystallization, *Polymer, vol. 12*, *Issue 3*, March 1971, p. 150-158.

[20] T. Ozawa, A New Method of Analyzing Thermogravimetric Data, *Bulletin of the chemical Society of Japan, 38*, 1965, p. 1881-1886.

[21] Z. H. Khan, S. A. Khan and M. A. Alvi, Study of Glass Transition and Crystallization Behavior in $Ga_{15}Se_{85-x}Pb_x$ ($0 \leq x \leq 6$) Chalcogenide Glasses, *ACTA PHYSICA POLONICA A, Vol. 123*, *No. 1,* 2013, p. 80-86.

[22] H. E. Kissinger, Reaction Kinetics in Differential Thermal Analysis, *Analytical Chemistry, Vol. 29*, *No. 11,* 1957, p. 1702-1706.

[23] K. Matusita, T. Konatsu, R. Yokota, Kinetics of non-isothermal crystallization process and activation energy for crystal growth in amorphous materials, *Journal of Material Science, vol. 19*, *No. 1*, 1984, p. 291-296.

[24] Praveen K. Jain, Deepika, K.S. Rathore, Nidhi Jain and N.S. Saxena, Activation Energy of Crystallization and Enthalpy Released of $Se_{90}In_{10-x}Sb_x$ (x=0, 2, 4, 6, 8, 10) Chalcogenide glasses. *Chalcogenide letters, Vol. 6, No. 3*, 2009, p. 97-107.

[25] T. Liu, N. Chen, Z. X. Xu, and R. Z. Ma, The amorphous-to-nanocrystalline transformation in $Fe_{73.5}Cu_1Nb_3Si_{13.5}B_9$ studied by thermogravimetry analysis, *Journal of Magnetism and Magnetic Materials, Vol. 152, Issue 3,* 1996, p. 359-364.